

Stability and electronic structure of *M*-DNA: Role of metal position

Simone S. Alexandre,^{1,*} Bernardo J. Murta,¹ José M. Soler,² and Félix Zamora³

¹*Departamento de Física, Universidade Federal de Minas Gerais, C.P. 702, 30123-970 Belo Horizonte, MG, Brazil*

²*Departamento de Física de la Materia Condensada, Universidad Autónoma de Madrid, ES-28049, Madrid, Spain*

³*Departamento de Química Inorgánica Universidad Autónoma de Madrid, ES-28049, Madrid, Spain*

(Received 11 March 2011; revised manuscript received 3 June 2011; published 6 July 2011)

We investigate, by first-principles density-functional calculations, fragments and periodic helices of CG- and AT-DNA, modified by incorporation of Zn^{2+} cations. We study the relative stability of different binding sites for the metal ions as well as different methods of charge neutralization. We find that binding the Zn cation to the N(7) atom of guanine or adenine leads always to lower energies than substitution of an imino proton between two H-bonded bases. Also, neutralizing with OH^- groups bonded to Zn^{2+} is more stable than removing protons from the phosphate groups. Contrarily to common wisdom, we find that planarity of the base pairs is not an essential factor of stability, and that nonplanar base pairs can also be stacked effectively. Finally, we find that the most stable CG and AT helices, with Zn^{2+} bonded to N(7) atoms and neutralized by OH^- ions, have wide band gaps of more than 2 eV, and we conclude that they are poor candidates for electronic conduction.

DOI: 10.1103/PhysRevB.84.045413

PACS number(s): 87.14.gk, 72.80.Le, 87.15.A—

I. INTRODUCTION

Construction of circuits based on molecules is the final goal of molecular electronics. Necessary components to achieve this end are molecular wires that fulfill two basic requirements: (i) a reasonably low resistance for charge transport and (ii) self-assembling capabilities to construct complex devices from basic building blocks. So far, there is not a single molecular wire that really fulfills both requirements. DNA has ideal structural capabilities,^{1–5} but it lacks a significant electrical conductivity.⁶ Many efforts are currently under way to enhance this property, but no clear improvements have been achieved yet. One approach, based on the selective biochemical insertion of metal ions between artificial nucleobases, is very tedious and still restricted in its extension⁷ (see Fig. 1).

Another method, the massive one-step insertion of metal ions, leads to the so-called *M*-DNA.¹⁰ This novel form of DNA presents controversial electrical properties^{10–12} and its structure is still a matter of debate.^{10,13–15} The first *M*-DNA structural model proposed by Lee *et al.*¹⁰ was based on preliminary NMR studies, which suggested that metal ions replace the imino proton in every base pair with a coordination that involves the C-G and A-T hydrogen bonds (see Fig. 2). However, more experimental data are still needed to confirm the whole structure.

Many experimental studies have been carried out involving metal ions and oligonucleotides.^{16–20} Exhaustive NMR and x-ray diffraction studies have been performed with many metal ions and different sequences of oligonucleotides.²¹ Most studies have concentrated specifically on structural models of interaction between the metal ions and the nucleobases, since these are the metal preferential targets rather than the phosphate groups or the sugar entities.¹⁶ The main result of these studies appears to be that the N(7) position at the guanine is the preferred binding site for transition metal ions in DNA at physiological pH. However, as *M*-DNA is typically formed at high pH values (between seven and nine, depending on the DNA sequence), this scenario still remains unclear, leaving other possibilities open for metal coordination to DNA.

In this context, several calculations have been carried out trying to gain insights into feasible *M*-DNA structures and their electronic structure.^{13–15} Fuentes-Cabrera *et al.*¹⁵ have compared several possibilities for the introduction of a Zn^{2+} cation in a DNA base pair, in a total of nine different structures. They address the geometric features and the stability of the different structures as well as the nature of their most relevant electronic states: the *d* bands of the Zn^{2+} cation, the highest-occupied molecular orbitals (HOMO), and the lowest-unoccupied molecular orbitals (LUMO). Among the models investigated, that previously proposed by some of us¹³ was the only one in which the Zn^{2+} cation was located at the major groove of the DNA chain. The stability of our geometry could not be directly compared with that of the other eight geometries examined in Ref. 15. However, the authors speculate that our structure may not be the most stable one because in a very stable complex known to form between Zn^{2+} and guanine the Zn ion is not in a cross-linked position (like in our proposed geometry) but it is rather bonded to the N(7) site. So, besides the possibility that the Zn^{2+} cation may prefer to be inserted in the minor groove, this speculation offers a different scenario for a more stable position of Zn^{2+} at the major groove.

Thus, in the present work, we compare three sites for the metal incorporation into DNA by: (a) replacing an imino hydrogen in the major groove (which will be referred to as model *a* in what follows), (b) replacing an imino hydrogen in the minor groove (model *b*), and (c) bounding to the N(7) of guanine or adenine (model *c*).

Unlike most previous *M*-DNA theoretical studies, we consider not only the monomers but also trimers and the periodic helix, so that the geometrical constraints imposed by the stacking of the base pairs are accounted for. Moreover, by introducing the chemical potential of water, we compare the energetics of all three models, despite the different number of water molecules present in them. Furthermore, we have also extended our studies to adenine-thymine DNA.

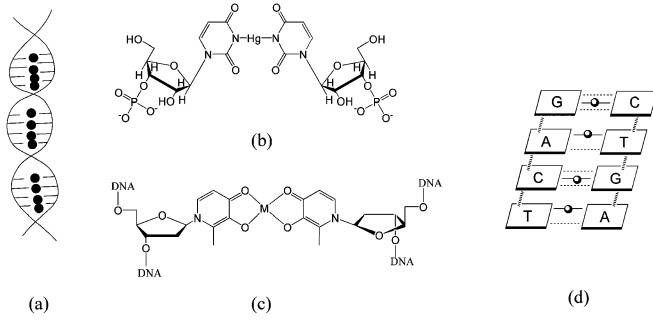


FIG. 1. Summary of several approaches to insert metal ions into DNA: (a) representation of the general concept, (b) a selected example of metal-ion-mediated base pairs with natural nucleosides,⁸ (c) a selected example that includes metal-ion-mediated base pairs with artificial nucleosides,⁹ and (d) schematic representation of the suggested structure of *M*-DNA.¹⁰

II. COMPUTATIONAL DETAILS

Our first-principles density-functional theory (DFT) simulations use the SIESTA code.²² Exchange and correlation effects are treated within the generalized gradient approximation.²³ We use norm-conserving pseudopotentials,²⁴ adding partial core corrections²⁵ for Zn. The basis set is made of double- ζ numerical pseudo-atomic orbitals^{22,26} with additional polarization functions in all atoms. We consider dry acidic DNA *in vacuo*, with protons as counterions in the phosphate groups, as in phosphoric acid. The geometries were optimized until the residual forces were smaller than 0.05 eV/Å. To simulate the periodic helical structures, we use the A form of DNA, favored under dry conditions, with a unit cell of eleven Zn-CG (Zn-AT) monomers containing 737–784 atoms, depending on the Zn²⁺ position and on the DNA base-pair type. Periodic boundary conditions were used in all directions, with enough empty space between the repeated chains to discard their interaction. These methods and parameters have been already applied successfully to investigate DNA properties.^{13,27}

III. RESULTS AND DISCUSSION

A. Structure and Stability

We start with monomers formed by a Zn²⁺ ion incorporated to one Watson-Crick CG and AT base-pair, including the corresponding segments of the sugar-phosphate backbones, with H atoms saturating the broken bonds at the extremes. The

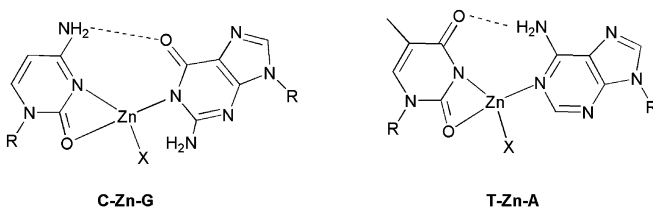


FIG. 2. Schematic models of base pairing for *M*-DNA, suggested by Lee *et al.*¹⁰

positions of these edge chain atoms, saturated by hydrogens, are not allowed to relax in order to mimic the geometric constraints in the periodic helix, so that these monomers can be used as units for the trimers and periodic systems in our study. Models are built with the Zn²⁺ cation replacing an imino proton in either the major or the minor grooves as well as bonded to the N(7) of G or A (models *a*–*c*). We have also attempted different methods of charge neutralization, by either removing protons from the phosphate groups or by adding OH[−] groups, within the geometrical constraints imposed by the stacking.

In order to investigate the effects of stacking on the relative stability of these structures, we build trimer fragments from the isolated monomers and we relax them with the methodology described in Ref. 13 to mimic the chain. In this procedure, the geometry optimization proceeds by relaxing the forces of the central monomer only while the remaining monomers are replicated from the central one, by helical translations-rotations, in each relaxation step. To generate the infinite periodic helix chains, the translation-rotation parameters of A-DNA are applied to the central base pair of the relaxed trimer without further relaxation.

Energy comparison between structures with a different number of water molecules is possible by introducing the chemical potential $\mu_{\text{H}_2\text{O}}$ for the water molecules in its liquid state or, equivalently, in its equilibrium vapor:

$$\mu_{\text{H}_2\text{O}} = E_{\text{H}_2\text{O}} + k_B T \log \left(\frac{P_v}{P_Q} \right) - k_B T \log Z_r. \quad (1)$$

$E_{\text{H}_2\text{O}}$ is the total energy of the molecule calculated with the same method and parameters used for *M*-DNA. P_v is the experimental vapor pressure of water at temperature T . P_Q is the quantum pressure: $P_Q = (M/2\pi\hbar^2)^{3/2} (k_B T)^{1/2}$, where M is the molecular mass. Z_r is the rotational partition function: $Z_r = (2\pi I_1 I_2 I_3)^{1/2} (k_B T / \hbar^2)^{3/2}$, where I_i is the i th moment of inertia. We ignore the internal vibrational free energy, since it is a minor component, and we assume that it will be relatively unaffected by the binding of the molecule to *M*-DNA where we are not considering it either.

In our calculations, we ignore all the vibrational degrees of freedom of the water molecules bound to *M*-DNA (and not only the internal ones) as well as their interaction with the rest of molecules in the liquid. Therefore, it might be argued that the last two terms of Eq. (1) that originate from those motions and interactions in the liquid should be also omitted. Thus omitting those terms is equivalent to assuming that the motion of water molecules and their interaction with the surrounding liquid are not affected by their binding to *M*-DNA. On the contrary, including them implies an assumption that those H₂O motions and interactions are completely absent when bound to *M*-DNA. The real value should be between these two extreme assumptions. Therefore, we will compare the relative free energies of the various *M*-DNA structures for a range of values of $\mu_{\text{H}_2\text{O}}$ that correspond to the inclusion (lower bound) or omission (upper bound) of those two terms whose values at $T = 293$ K are −0.42 and −0.09 eV, respectively.

In order to obtain charge neutrality, we proceed in two different ways: (i) neutralizing by adding hydroxyl groups;

one hydroxyl group, in addition to one neutral water molecule, is added when the metal ion is in a cross-linked position at the major or minor grooves, replacing an imino proton (models *a* and *b*). In this way, we generate a total of eight structures, depending on DNA type (CG or AT), metal position (major or minor groove), and relative positions of the water molecule and the hydroxyl group. For Zn^{2+} bonded to N(7) (model *c*), we add two hydroxyl groups and one water molecule, generating three structures with different relative positions between the water molecule and the hydroxyl, for each DNA type. (ii) Neutralizing by removing protons from the phosphate group; one proton was removed in models *a* and *b* and two protons were removed in model *c*. Given that each monomer has four phosphate protons, there are four ways of removing one proton and six ways of removing two protons. However, we discarded removing two protons from the phosphate group of the same base since this lead to very unfavorable structures. Thus we considered a total of four structures for each model, totalizing twelve structures for each DNA type. In each case, a tetrahedral coordination environment of Zn was completed with neutral water molecules.

The energy comparison, after geometry optimization, indicates that neutralizing with hydroxyl groups is always more favorable than removing protons from the phosphate. This can be justified by the shorter resulting distance between the positive and negative charges. Figure 3 shows the schematic representation of the structures of lowest energy for the three different Zn^{2+} positions in CG and AT monomers. We denote the monomers of models *a*, *b*, and *c* as $(\text{CG})_1^{a,b,c}$ and $(\text{AT})_1^{a,b,c}$. Correspondingly, $(\text{CG})_3^{a,b,c}$ and $(\text{AT})_3^{a,b,c}$ denote the trimers, and $(\text{CG})_\infty^{a,b,c}$ and $(\text{AT})_\infty^{a,b,c}$ are the periodic helices.

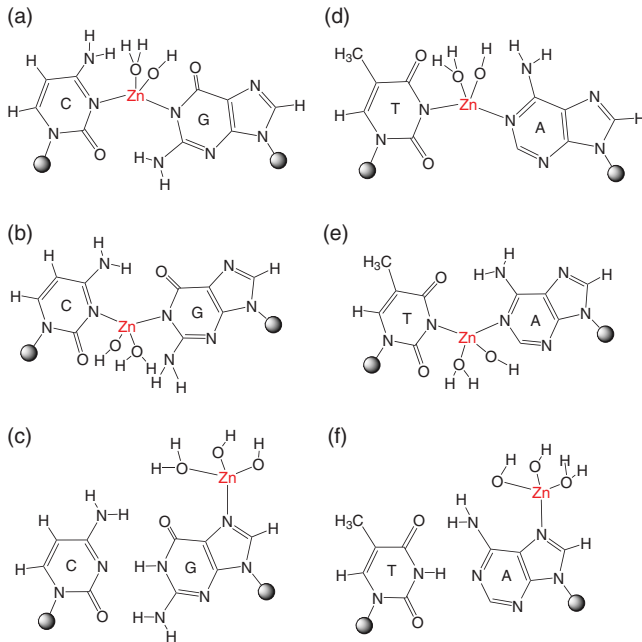


FIG. 3. (Color online) Schematic structure of monomers with the lowest energy for the three different Zn positions: (a) $(\text{CG})_1^a$, (b) $(\text{CG})_1^b$, (c) $(\text{CG})_1^c$, (d) $(\text{AT})_1^a$, (e) $(\text{AT})_1^b$, and (f) $(\text{AT})_1^c$.

TABLE I. Relative energies per base pair (in eV) of the Zn^{2+} -CG and Zn^{2+} -AT monomers, trimers, and helices in their lowest energy structures for each metal position considered. The structures in which the Zn is bound to the N(7) of the guanine (adenine) at the major groove (*c* model) are energetically more stable for both CG and AT structures and their total energies are used as reference.

Structure	ΔE	Figure	Structure	ΔE	Figure
$(\text{CG})_1^c$	0.00	3c	$(\text{AT})_1^c$	0.00	3f
$(\text{CG})_1^a$	0.52	3a	$(\text{AT})_1^a$	0.97	3d
$(\text{CG})_1^b$	1.15	3b	$(\text{AT})_1^b$	1.31	3e
$(\text{CG})_3^c$	0.00	4c	$(\text{AT})_3^c$	0.00	4f
$(\text{CG})_3^a$	1.33	4a	$(\text{AT})_3^a$	0.21	4d
$(\text{CG})_3^b$	1.26	4b	$(\text{AT})_3^b$	0.85	4e
$(\text{CG})_\infty^c$	0.00	5c	$(\text{AT})_\infty^c$	0.00	5f
$(\text{CG})_\infty^a$	2.44	5a	$(\text{AT})_\infty^a$	1.84	5d
$(\text{CG})_\infty^b$	2.66	5b	$(\text{AT})_\infty^b$	1.90	5e

The formation energies of the *a* and *b* models, relative to the *c* model, are calculated as

$$\Delta E^{a,b} = E_{\text{tot}}^{a,b} - E_{\text{tot}}^c - (N_{\text{H}_2\text{O}}^{a,b} - N_{\text{H}_2\text{O}}^c)\mu_{\text{H}_2\text{O}}, \quad (2)$$

where E_{tot}^i and $N_{\text{H}_2\text{O}}^i$ are the *ab initio* total energy and the number of water molecules of the *i*th structure ($i = a, b, c$), and $\mu_{\text{H}_2\text{O}}$ is the chemical potential of water defined in Eq. (1). This definition allows to compare structures with different numbers of water molecules to that of the most stable *c* model. The energies of the $(\text{CG})_1^a$ and $(\text{CG})_1^b$ monomers can be compared directly because they both have a missing imino proton and the same number of hydroxyl and water molecules. However, they have, nominally, one less water molecule than model *c* because the latter has kept the imino proton that is absent in models *a* and *b* and an additional OH group that has been added for charge neutralization. We find that $(\text{CG})_1^c$ is more stable. The energies of these two models are presented in Table I relative to that of $(\text{CG})_1^c$. This does not rule out the possibility that one or more of the models investigated in Ref. 15, with Zn in the minor groove, might be more stable than our $(\text{CG})_1^a$ geometry.

For the CG monomers, we find that the formation energies of the three structures are ordered as $E_1^c < E_1^a < E_1^b$. We observe the same ordering for the AT monomers, with the difference that, in this case, the relative positions of the water and hydroxyl group of the *c* model change when compared with those of the CG monomers.

For the $(\text{CG})_3^a$ model, we tested the following configurations: (1) with each base pair having all the OH^- and water molecules as in the monomer in Fig. 3(a) and two water molecules per trimer unbind spontaneously from the DNA during the minimization; (2) with two water molecules saturating the Zn^{2+} cation, and its charge neutralized by removing one proton from each phosphate group. Two water molecules are also lost during the optimization process. Furthermore, this structure winds up with a higher energy than the previous one, and (3) our previously proposed model, shown in Fig. 4(a) in which OH^- ions form a bridge between two zinc atoms. In order to compare its energy with that of (1) and (2), we use Eq. (2). We find that our model has an energy

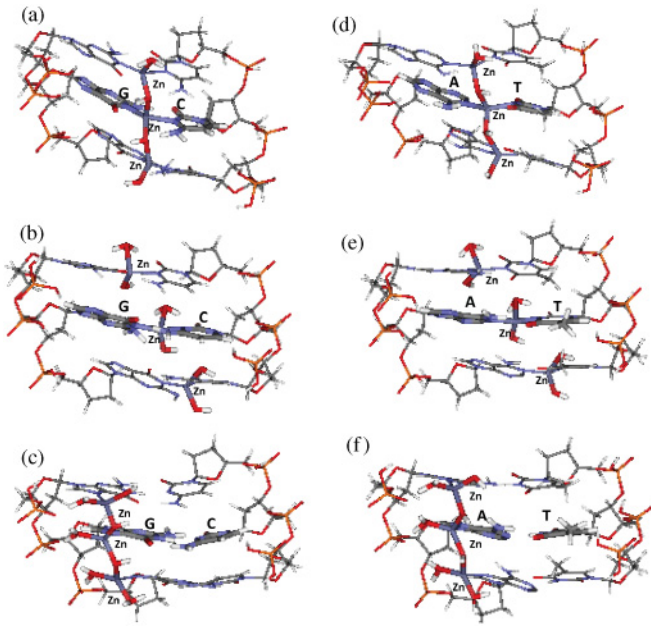


FIG. 4. (Color online) Optimized geometries of trimers with lowest energy for the three different Zn positions: (a) $(CG)_3^a$, (b) $(CG)_3^b$, (c) $(CG)_3^c$, (d) $(AT)_3^a$, (e) $(AT)_3^b$, and (f) $(AT)_3^c$.

1.53 and 1.65 eV/base-pair lower than that of models (1) and (2) for CG-DNA, respectively. For AT-DNA, the energy of (3) is also lower than that of (1) and (2) by 1.57 and 1.73 eV/pair, respectively.

For the $(CG)_3^b$ and $(AT)_3^b$ models we also find that neutralizing with OH^- groups, bonded to the Zn^{2+} cations, leads to energies of 1.22 and 1.41 eV (per base pair) lower than in the model that removes protons from the phosphate groups, respectively. However, the OH^- groups do not form a zigzag chain connecting the metal ions, like in the *a* and *c* models, because of the larger distance between them [see Figs. 4(b) and 4(e)].

For the $(CG)_3^c$ and $(AT)_3^c$ models, we considered models where the Zn cations were saturated with H_2O and neutralized by removal of one proton from each of the two phosphate groups. We also generated chains where each Zn cation is saturated by two OH groups, one of them shared by two Zn cations of adjacent base pairs. During relaxation of the latter models, one proton from the phosphate group of each base pair migrates to neutralize one of the OH groups, forming a water molecule, as shown in Figs. 4(c) and 4(f). In this case, charge neutralization occurs partially in the Zn and partially in the phosphate, and the minimized energy is lower by about 2.00 eV per base pair than neutralizing by removal of two protons from the phosphate groups.

Figure 5 shows the relative formation energies as a function of the chemical potential of water. Within the range of values explained previously, we find that the energy ordering of models *a* and *b* depends on the chemical potential but model *c* is always the most stable one for all values of μ_{H_2O} .

Concerning the structural distortion produced by metal incorporation, we examine the planarity of the relaxed geometries, an issue emphasized in previous studies,^{14,15} where it was claimed that planar base pairs would be necessary to build an

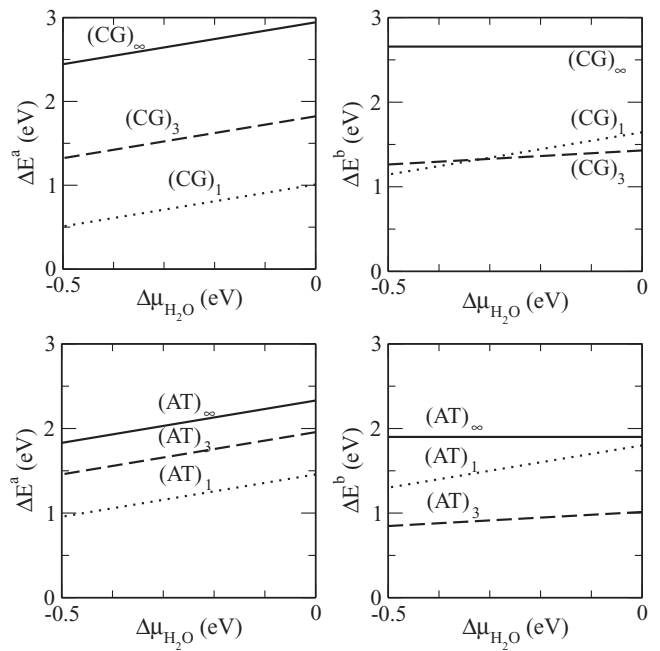


FIG. 5. Relative energies, given by Eq. (2) of models *a* (left panels) and *b* (right panels), relative to those of model *c*, as a function of the effective chemical potential of water given by Eq. (1) with $\Delta\mu_{H_2O} = \mu_{H_2O} - E_{H_2O}$. The lower limit ($\Delta\mu_{H_2O} = -0.5$ eV) corresponds to assuming that water molecules bonded to Zn-DNA cannot move nor interact with other water molecules. The upper limit ($\Delta\mu_{H_2O} = 0$) corresponds to making an assumption that their motions and interactions are not affected by their binding to Zn-DNA (see text for further explanations). The three models are shown schematically in Fig. 3.

extended helix. However, in our previous work¹³ we found that the metal cations prefer to be in a tetrahedral configuration, distorting the helix.

As two planarity indicators, we study the angle between the average planes of the two corresponding nucleobases (G and C, or A and T) and the dihedral angle between their most significant atoms.¹⁴

The structural data collected in Table II clearly show that the structures undergo a significant change in planarity by coordination of the metal ion. The distortion is weak only in the models with Zn^{2+} coordinated to the N(7) of guanine or adenine. Indeed, the nonplanarity is mainly related to the simultaneous coordination of the metal ion to both nucleobases. Thus the largest distortions occur in the models *a* and *b* in which the metal ions replace imino protons of the nucleobases. These are the typical metal-ion locations of the so-called Lee model (scheme 1). The increase of dihedral angle is most dramatic in $(CG)_1^a$. In contrast, in $(CG)_1^c$ the coordination of $Zn(II)$ at the N(7) of guanine barely affects the planarity (angle of only 0.61° between the average nucleobase planes) while the distances and angles of the three C-G H-bonds are only slightly affected. The geometrical distortions increase dramatically in the trimers, even for the *c* models, since they have to stack the Zn^{2+} ions and their OH^- counterions and H_2O saturators, constrained also by the sugar-phosphate backbone.

TABLE II. Summary of structural parameters of the relaxed models.

Structure	(deg) ^a	(deg) ^b	l_i (Å) ^{c,d,e}	a_i (deg) ^{f,g,h}	l_{M-B} (Å) ⁱ	H-bonds ^j
(CG) ₁ ^a	20.97	168.49	4.504	34.87	1.952 [N1 ^G]	W1-N4
			3.764	148.08	1.963 [N3 ^C]	W2-N4
			3.002	169.42		W1-O6 W2-O6
(CG) ₁ ^b	17.63	-174.51	2.767	167.98	1.958 [N1 ^G]	W-O2
			3.704	138.95	1.996 [N3 ^C]	W-N2
			4.560	111.90		OH-N2
(CG) ₁ ^c	0.61	179.99	2.786	178.40	2.002 [N7 ^G]	W-O6
			2.822	178.41		
			2.736	178.06		
(CG) ₃ ^a	19.41	-177.44	4.900	137.53	1.987 [N1 ^G]	OH1-N4
			3.770	131.26	2.151 [N3 ^C]	OH2-O6
			2.846	171.96	2.475 [O6 ^G]	
(CG) ₃ ^b	22.96	-159.59	2.580	166.00	1.936 [N1 ^G]	W-O2
			3.674	138.18	1.997 [N3 ^C]	W-N2
			4.819	119.11		OH-N2
(CG) ₃ ^c	22.09	174.94	2.764	172.30	2.062 [N7 ^G]	
			2.829	170.88		
			2.833	177.85		
(AT) ₁ ^a	3.57	36.88	5.046	136.29	2.033 [N1 ^A]	W-O4
			3.790	141.83	1.977 [N3 ^T]	OH-N6
			2.699	173.71	2.014 [N1 ^A]	W-O2
(AT) ₁ ^b	22.70	52.00	3.640	131.98	1.981 [N3 ^T]	OH-C2
			2.820	178.0	1.975 [N7 ^A]	OH-O6
			2.751	178.9		
(AT) ₃ ^a	34.33	4.01	5.311	145.67	2.083 [N1 ^A]	OH-O6
			3.576	124.41	1.959 [N3 ^T]	
			2.739	166.76	1.986 [N1 ^A]	W-O2
(AT) ₃ ^b	16.54	45.43	3.629	134.76	1.950 [N3 ^T]	OH-O2
			2.806	176.77	2.027 [N7 ^A]	
			2.762	170.57		

^a a : angle between the average planes of the two nucleobases.^b d : dihedral angle C4^C-N3^C-N1^G-C2^G or C4^T-O4^T-N1^A-C2^A.^c l_1 : bond length O6^G-N4^C or N6^A-O4^T.^d l_2 : bond length N1^G-N3^C or N1^A-N3^T.^e l_3 : bond length N2^G-O2^C.^f a_1 : bond angle O6^G-H-N4^C or N6^A-H-O4^T.^g a_2 : bond angle N1^G-H-N3^C or N1^A-H-N3^T.^h a_3 : bond angle N2^G-H-O2^C.ⁱ l_{M-B} : bond length between metal and nucleobase atoms.^jH-bonds: hydrogen bonds between water (W) or OH molecules, coordinated to Zn(II), and nucleobase atoms.

The decreased planarity leads to the breaking of some H-bonds between the two base pairs and to large distortions in those remaining, as observed in the values of distances and angles collected in Table II. Two effects are expected and observed: (i) metal ions coordinated to N(7) sites of guanine or adenine typically increase the strength of the hydrogen bonds between base pairs²⁸ and (ii) metal ions replacing imino protons between the Watson-Crick base pairs increase the binding between the two bases. To estimate the effects in the H bonds, we have focused on the distance between donor and acceptor atoms and on the angle between donor-H-acceptor atoms. In addition, we include in Table II the angle N3C-H-N1G or N3T-H-N1A along with its equivalents N1G-Zn-N3C and N1A-Zn-N3T in the metalated pair bases.

Other interesting features are related to the presence of water molecules and of hydroxyl groups coordinated to Zn(II). We observe the formation of new H bonds between these groups coordinated to the metal ion and the nucleobases. Thus a new H bond is formed between N4C and O6G and hydroxyl groups in (CG)₃^a, and four new H bonds are formed in (CG)₃^b between the nucleobases, the water, and hydroxyl groups.

In our models, the Zn(II) ion presents a tetrahedral geometry with severe distortions of planarity and linearity. The exception to this rule is (CG)₃^a, in which an additional Zn-guanine bond is formed (with the O6G) leading to a highly distorted penta-coordinated environment of the metal ion. No clear correlation between the calculated energies and the planarity of the models can be found. However, we find that when the

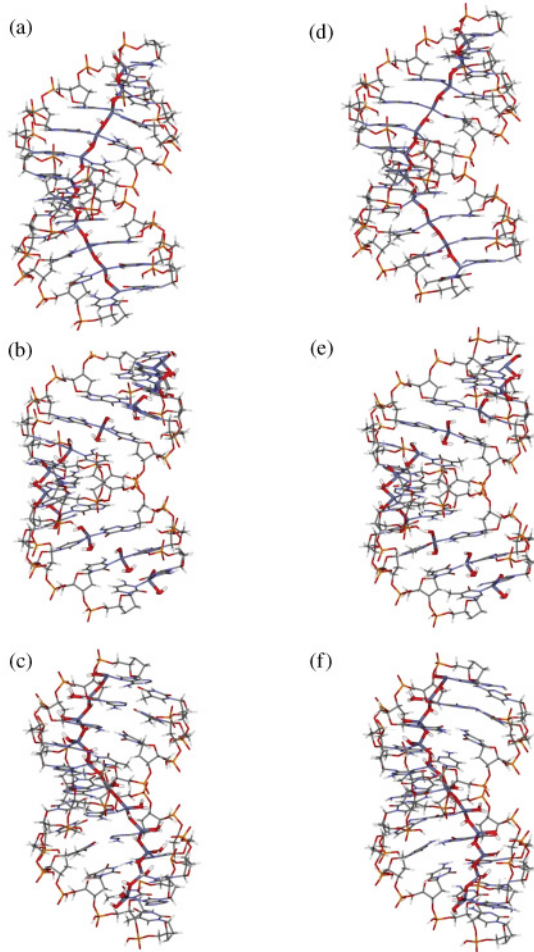


FIG. 6. (Color online) Global view of the Zn-DNA helices: (a) $(CG)_{\infty}^a$, (b) $(CG)_{\infty}^b$, (c) $(CG)_{\infty}^c$, (d) $(AT)_{\infty}^a$, (e) $(AT)_{\infty}^b$, and (f) $(AT)_{\infty}^c$.

Watson-Crick H bonds between the base pairs are retained the resulting structure is always the most stable one. This is attained by the N(7) metal coordination and, therefore, the results suggest that the N(7) coordination is the most favorable situation. Somehow, surprisingly, the coordination of Zn(II) to the major groove is energetically more stable than the coordination to the minor groove.

B. Electronic Structure

We now turn to the electronic structure, and we analyze the effects of the metal position on the band structure and the conductivity of the periodic Zn-DNA chains shown in Fig. 6. The band structure for each case is shown in Fig. 7. We observe that the insertion of the metal cation affects the band gap strongly only in the model *a* for both CG and AT DNA. In the case of CG DNA the gap is strongly reduced from 1.98 eV in the pristine case to 0.48 eV for the $(CG)_{\infty}^a$ system, as previously reported.¹³ For the $(AT)_{\infty}^a$ DNA model the effect is not as strong, with a decrease from 3.13 to 2.44 eV, but this is still a substantial gap reduction when compared with the cases of the *b* and *c* models where gaps are reduced by ~ 0.25 eV at most.

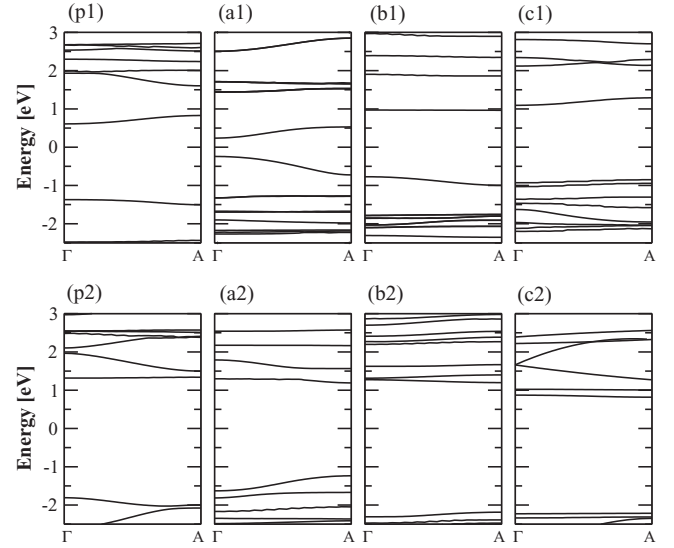


FIG. 7. Band structures of: (p1) pristine CG-DNA, (a1) $(CG)_{\infty}^a$, (b1) $(CG)_{\infty}^b$, (c1) $(CG)_{\infty}^c$, (p2) pristine AT-DNA, (a2) $(AT)_{\infty}^a$, (b2) $(AT)_{\infty}^b$, and (c2) $(AT)_{\infty}^c$.

Regarding the dispersions of the HOMO and LUMO bands, the most systematic pattern is their enhancement in the *a* model for both CG and AT DNA. This effect is connected with the enhanced overlap of the base pairs along the chain due to the stacking geometry in this model. This would point to lower effective masses and enhanced carrier mobilities for the *a* model should doping of the *M*-DNA chains be achieved. Clearly, this would only have an impact on charge conduction in *M*-DNA in a scenario where band transport is the proper description of charge transport in these systems,^{29–34} and even so, the nature of scattering mechanisms must be addressed before any definitive conclusions can be drawn.

IV. CONCLUSIONS

In conclusion, we have studied the structural and electronic properties of Zn-DNA complexes proposed as molecular conductors. We conclude that the N(7) site at the guanine (adenine) is the most stable binding site for insertion of Zn^{2+} at CG (AT) DNA, and that it is more effectively neutralized by OH^- ions than by removing protons from the DNA phosphates. Finally, in our previous study, we came to the conclusion that Zn-DNA, with the Zn cation at the major groove, would be a promising candidate as a basis for conducting *M*-DNA systems. However, in the present work the identification of the more stable N(7) site, showing a large electronic HOMO-LUMO gap, leads us to revise that statement.

ACKNOWLEDGMENTS

This work has been supported by Brazilian agencies: Fapemig, CNPq, and Ministério da Ciência e Tecnologia; by Grants FIS2009-12712, MAT2010-20843-C02-01, and CSD2007-00050 of the Spanish Ministry of Science and Innovation; and by European Grant EU(FP6-029192).

*simoni@fisica.ufmg.br

- ¹J. P. Zheng, J. J. Birktoft, T. W. Y. Chen, R. Sha, P. E. Constantinou, S. L. Ginell, C. Mao, and N. C. Seeman, *Nature (London)* **461**, 74 (2009).
- ²N. C. Seeman, *Nature (London)* **421**, 427 (2003).
- ³M. Niemeyer, *Angew. Chem. Int. Ed.* **40**, 4128 (2001).
- ⁴S. M. Douglas, H. Dietz, T. Liedl, B. Hogberg, F. Graf, and W. M. Shih, *Nature (London)* **459**, 414 (2009).
- ⁵H. Dietz, S. M. Douglas, and W. M. Shih, *Science* **325**, 725 (2009).
- ⁶D. Porath, G. Cuniberti, and R. D. Felice, *Top. Curr. Chem.* **237**, 183 (2004).
- ⁷J. Mueller, *Eur. J. Inorg. Chem.* **2008**, 3749 (2008).
- ⁸Y. Tanaka, S. Oda, H. Yamaguchi, Y. Kondo, C. Kojima, and A. Ono, *J. Am. Chem. Soc.* **129**, 244 (2007).
- ⁹K. Tanaka, A. Tengeiji, T. Kato, N. Toyama, M. Shiro, and M. Shionoya, *J. Am. Chem. Soc.* **124**, 12494 (2002).
- ¹⁰J. S. Lee, L. J. P. Latimer, and R. S. Reid, *Biochem. Cell. Biol.* **71**, 162 (1993).
- ¹¹R. Mas-Balleste, O. Castillo, P. J. S. Miguel, D. Olea, J. Gomez-Herrero, and F. Zamora, *Eur. J. Inorg. Chem.* **2009**, 2885 (2009).
- ¹²K. Mizoguchi, S. Tanaka, T. Ogawa, N. Shiobara, and H. Sakamoto, *Phys. Rev. B* **72**, 033106 (2005).
- ¹³S. S. Alexandre, J. M. Soler, L. Seijo, and F. Zamora, *Phys. Rev. B* **73**, 205112 (2006).
- ¹⁴G. Brancolini and R. D. Felice, *J. Phys. Chem. B* **112**, 14281 (2008).
- ¹⁵M. Fuentes-Cabrera, B. G. Sumpter, J. E. Sponer, J. Sponer, L. Petit, and J. C. Wells, *J. Phys. Chem. B* **111**, 870 (2007).
- ¹⁶B. Lippert, *Coordin. Chem. Rev.* **200**, 487 (2000).
- ¹⁷E. C. Fusch and B. Lippert, *J. Am. Chem. Soc.* **116**, 7204 (1994).
- ¹⁸F. Zamora and M. Sabat, *Inorg. Chem.* **41**, 4976 (2002).
- ¹⁹P. Amo-Ochoa, S. S. Alexandre, C. Pastor, and F. Zamora, *J. Inorg. Biochem.* **99**, 2226 (2005).
- ²⁰P. Amo-Ochoa, O. Castillo, P. J. S. Miguel, and F. Zamora, *J. Inorg. Biochem.* **102**, 203 (2008).
- ²¹E. Sletten and N. Froystein, *Met. Ions Biol. Syst.* **32**, 397 (1996).
- ²²J. M. Soler, E. Artacho, J. D. Gale, A. Garcia, J. Junquera, P. Ordejon, and D. Sanchez-Portal, *J. Phys. Condens. Matter* **14**, 2745 (2002).
- ²³J. P. Perdew, K. Burke, and M. Ernzerhof, *Phys. Rev. Lett.* **77**, 3865 (1996).
- ²⁴N. Troullier and J. L. Martins, *Phys. Rev. B* **43**, 1993 (1991).
- ²⁵S. G. Louie, S. Froyen, and M. L. Cohen, *Phys. Rev. B* **26**, 1738 (1982).
- ²⁶O. F. Sankey and D. J. Niklewski, *Phys. Rev. B* **40**, 3979 (1989).
- ²⁷P. J. de Pablo, F. Moreno-Herrero, J. Colchero, J. Gomez-Herrero, P. Herrero, A. M. Baro, P. Ordejon, J. M. Soler, and E. Artacho, *Phys. Rev. Lett.* **85**, 4992 (2000).
- ²⁸B. Lippert, *Prog. Inorg. Chem.* **54**, 385 (2005).
- ²⁹K.-H. Yoo, D. H. Ha, J.-O. Lee, J. Park, J. Kim, J. Kim, H.-Y. Lee, T. Kawai, and H. Y. Choi, *Phys. Rev. Lett.* **87**, 198102 (2001).
- ³⁰S. Komineas, G. Kalosakas, and A. R. Bishop, *Phys. Rev. E* **65**, 061905 (2002).
- ³¹G. Triberis, C. Simserides, and V. Karavolas, *Condens. Matter* **17**, 2681 (2005).
- ³²S. Rakhmanova and E. Conwel, *J. Phys. Chem. B* **105**, 2056 (2001).
- ³³W. Zhang, A. O. Govorov, and S. E. Ulloa, *Phys. Rev. B* **66**, 060303 (2002).
- ³⁴S. S. Alexandre, E. Artacho, J. M. Soler, and H. Chacham, *Phys. Rev. Lett.* **91**, 108105 (2003).